

⁵⁷Fe Mössbauer spectroscopy study of a 2D spin transition coordination polymer built from a tris-1R-tetrazole ligand

N. N. Adarsh¹ · Marinela M. Dîrtu¹ · Aurelian Rotaru² · Yann Garcia¹ 

© Springer International Publishing AG 2017

Abstract [Fe{N(entz)₃}₂](ClO₄)₂ (N(entz)₃ = tris(2-(1H-tetrazol-1-yl)ethyl)-amine) is a 2D Fe^{II} coordination polymer built from a tris-1-R tetrazole building block. This thermochromic Fe^{II} complex which was investigated by variable temperature ⁵⁷Fe Mossbauer spectroscopy (78–300 K) displays on cooling a complete, abrupt and hysteretic spin transition at $T_c^\uparrow = 170(1)$ K and $T_c^\downarrow = 149(1)$ K. The reversibility of the spin transition over several thermal cycles was deduced from SQUID magnetometry. Differential scanning calorimetry reveals a reversible first order phase transition on cooling below room temperature, with entropy data consistent with the highly cooperative character of the spin transition.

Keywords ⁵⁷Fe Mossbauer spectroscopy · Coordination polymers · Spin transition · Tetrazole · Molecular bistability

1 Introduction

There is currently a great scope of investigation on tetrazole coordination polymers (CPs) mostly for their fluorescence, energetic, porous and magnetic properties. In particular spin crossover (SCO) phenomena [1] were observed for multidimensional (1D, 2D and 3D) Fe^{II}

This article is part of the Topical Collection on *Proceedings of the 3rd Mediterranean Conference on the Applications of the Mössbauer Effect (MECAME 2017), Jerusalem, Israel, 5–7 June 2017*
Edited by Mira Ristic, Stjepko Krehula, Israel Nowik and Israel Felner

✉ Yann Garcia
yann.garcia@uclouvain.be

¹ Institute of Condensed Matter and Nanosciences, Molecules, Solids and Reactivity (IMCN/MOST), Université catholique de Louvain, Place L. Pasteur 1, 1348 Louvain-la-Neuve, Belgium

² Department of Electrical Engineering and Computer Science & Research Center MANSiD, “Stefan cel Mare” University, University Street, No. 13, Suceava 720229, Romania

tetrazole and triazole CPs, and recently reviewed [2]. Such materials continue to attract growing interest, e.g. for their potential in pressure sensor devices [3, 4]. 2D CPs are interesting due to the possibility to offer guest insertion and controlled SCO cooperative effects. Limited examples of 2D Fe^{II} SCO bis-azole CPs have been however described. This involves: bis-1,2,4-triazole [5–7], bis-1,2,3-triazole [8, 9], bis-1R-tetrazole [10], bis-2R-tetrazole ligands [11, 12], and even a combination of bis-1,2,3-triazole and 1R-tetrazole ligand [13]. While the first example of a 2D Fe^{II} SCO CP built from a 1R-tetrazole ligand was reported by Rudolf et al. in 1996 using the spider like ligand, **N(entz)₃** = tris(2-(1H-tetrazol-1-yl)ethyl)-amine [14], more recent examples were found with tris-tetrazole ligands [15, 16]. Indeed, [Fe{**N(entz)₃**}₂](BF₄)₂ (**1**) was shown to display an abrupt, complete and hysteretic spin transition at $T_c^\uparrow = 176$ K and $T_c^\downarrow = 167$ K as concluded from ⁵⁷Fe Mössbauer spectroscopy [14]. In the present work, we prepared and characterized, a new CP, namely [Fe{**N(entz)₃**}₂](ClO₄)₂ (**2**) whose SCO properties were investigated by magnetometry, ⁵⁷Fe Mössbauer and differential scanning calorimetry.

2 Experimental

Tris(2-(1H-tetrazol-1-yl)ethyl)-amine ligand (**N(entz)₃**) was synthesized using tris(2-aminoethyl)-amine following a reported procedure [17]. **2** was synthesized by mixing acetonitrile solution (6 mL) of **N(entz)₃** (100 mg, 0.328 mmol) and Fe(ClO₄)₂·6H₂O (42 mg, 0.165 mmol) with a pinch of ascorbic acid in a vial, which was further sonicated for 10 min to afford a white precipitate. Yield: 77% (110 mg, 0.127 mmol). Anal. Calcd for C₁₈H₃₀Cl₂N₂₆O₈Fe (%): C, 24.98; H, 3.49; N, 42.08. Found: C, 25.46; H, 3.65; N, 42.52. Mössbauer spectra were recorded in transmission geometry using a Wissel GmbH spectrometer equipped with a Cyclotron Ltd ⁵⁷Co(Rh) source operating at room temperature, and fitted to an Oxford Instruments Optistat bath cryostat for variable temperature measurements. Spectra were fitted to a sum of Lorentzians by least-squares refinement using Recoil 1.05 Mössbauer Analysis Software [18]. All isomer shifts and quadrupole splittings are given with respect to α -iron calibration at room temperature. Magnetic susceptibilities were measured in the temperature range 4–300 K using a Magnetic Property Measurement System (MPMS[®]3) SQUID magnetometer operating at 1000 Oe. Data were corrected for magnetization of the sample holder and diamagnetic contributions, which were estimated from the Pascal constants. Differential scanning calorimetry measurements were carried out in a He(g) atmosphere using a Perkin-Elmer DSC Pyris instrument equipped with a liquid nitrogen cryostat operating down to 108 K and an integration module for specific heat determination [19].

3 Results and discussion

Upon quench cooling to liquid nitrogen, a dramatic colour change from white to violet was observed (Fig. 1a) precluding a thermally induced SCO from Fe^{II} high-spin (HS) to Fe^{II} low-spin (LS). The SCO behaviour of **2** was confirmed by variable-temperature magnetization data recorded over the range 80–250 K, with a scan rate of 2 K min⁻¹ between each data points in order to avoid significant thermal kinetic effects. At room temperature $\chi_M T$ is equal to 3.72 cm³ mol⁻¹ K, in agreement with a full fraction of Fe^{II} ions in the HS state. As T is lowered, $\chi_M T$ first decreases very slowly to 188 K and then rapidly down to 100 K.

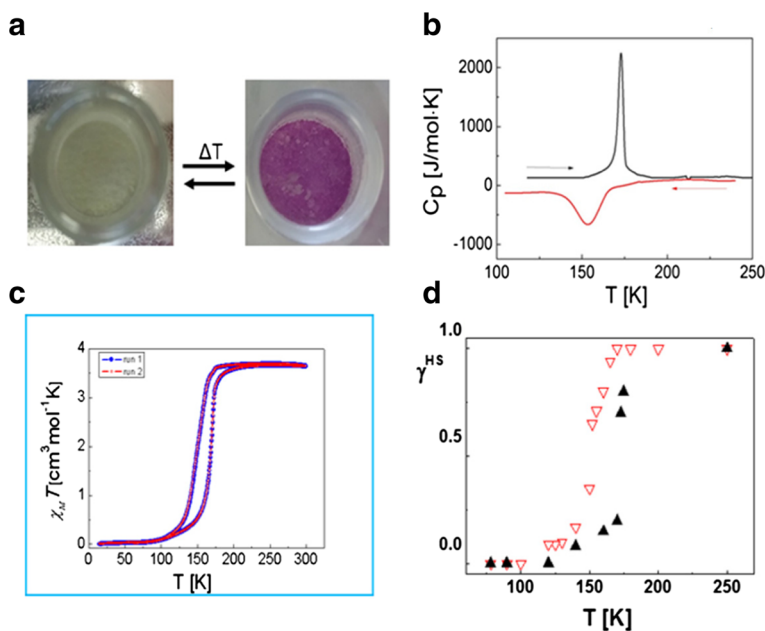


Fig. 1 **a** Thermochromism from white (at room temperature) to violet (at liquid nitrogen temperature) of **2**; **b** C_p vs. T for **2** on warming and cooling at $10 \text{ K} \cdot \text{min}^{-1}$ over the range 108–250 K; **c** $\chi_M T$ vs. T for **2** for two thermal cycles, obtained from SQUID data; **d** γ^{HS} vs. T as deduced from Mössbauer spectroscopy for **2**

As the temperature is increased back, $\chi_M T$ does not follow the same pathway, thereby displaying a hysteresis loop of width $\sim 22 \text{ K}$, centred at 160 K. The transition temperatures are $T_c^\uparrow = 170 \text{ K}$ and $T_c^\downarrow = 148 \text{ K}$. This hysteresis is retained over successive cooling and heating thermal cycles (Fig. 1c).

Temperature dependent ^{57}Fe Mössbauer spectra of **2** were recorded over the range 78–298 K. At 78 K, the spectrum of **2** consists of a single quadrupole doublet corresponding to a LS Fe^{II} ion, with an isomer shift $\delta^{\text{LS}} = 0.59(1) \text{ mm} \cdot \text{s}^{-1}$ and a low quadrupole splitting $\Delta E_Q^{\text{LS}} = 0.21(1) \text{ mm} \cdot \text{s}^{-1}$ (Fig. 2). This quadrupole splitting is characteristic for a lattice contribution to the electric field gradient which indicates a low distortion of the LS octahedron in **2**. Upon warming up to 135 K, no change is observed in the spectra but at 140 K, a new quadrupole doublet characteristics of a HS Fe^{II} ion is detected, indicating the onset of a SCO from LS to HS, which progresses further at 175 K. Indeed, from 250 K and up to room temperature, no LS fraction is detected in agreement with the white color of the powder, which is characteristic of the HS state for such materials. Indeed, at 298 K, a single HS quadrupole doublet is observed, with $\delta^{\text{HS}} = 1.07(1) \text{ mm/s}$ and $\Delta E_Q^{\text{HS}} = 1.46(1) \text{ mm/s}$, indicating a complete and abrupt SCO. On cooling back to 78 K, a hysteretic behaviour is clearly revealed, by comparing Mössbauer spectra recorded at 160 K (Fig. 1). The observed hyperfine parameters are in good agreement with the ones observed for **1** [14] (Table 1).

After evaluation of the area fraction, the HS molar fraction, γ_{HS} , was calculated assuming equal Lamb Mössbauer factors for HS and LS ions. This hypothesis is realistic when dealing with sharp spin transitions as concluded from the plot of the area fraction vs T [20]. As a result, the SCO curve is shown to reveal an abrupt transition with a hysteresis width

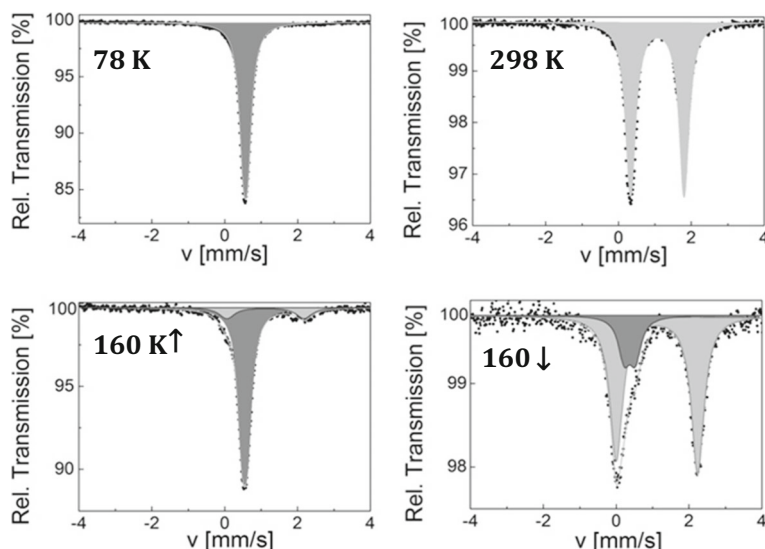


Fig. 2 Selected ^{57}Fe Mössbauer spectra for **2** showing the hysteretic behaviour of the spin transition. Grey and dark grey correspond to the HS and LS doublets, respectively

Table 1 Overview of selected ^{57}Fe Mössbauer parameters for **2**

T [K]	$A_{\text{HS}}/A_{\text{tot}}$ [%]	HS [mm/s]			LS [mm/s]		
		Δ	ΔE_Q	$\Gamma/2$	Δ	ΔE_Q	$\Gamma/2$
78(1)	0	–	–	–	0.59(1)	0.21(1)	0.14(1)
160(1) \uparrow	15	1.12(1)	2.20(1)	0.20(1)	0.55(1)	0.14(1)	0.15(1)
298(1)	100	1.07(1)	1.46(1)	0.16(1)	–	–	–
160(1) \downarrow	81	1.12(1)	2.23(1)	0.21(1)	0.57(1)	0.13(1)	0.16(1)

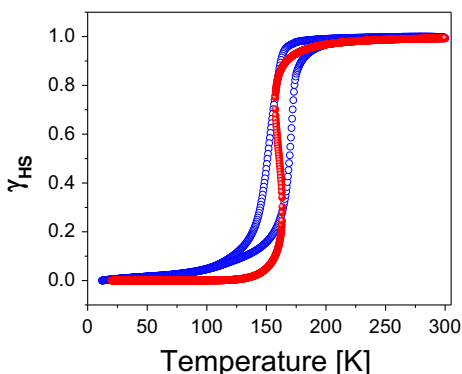
δ : isomer shift (with respect to α -Fe at 298 K); ΔE_Q : quadrupole splitting; $\Gamma/2$: half width at half maximum

of 20 K (Fig. 1d). The transition temperatures, on warming and cooling, are $T_c^\uparrow = 170(1)$ K and $T_c^\downarrow = 149(1)$ K, respectively.

Differential scanning calorimetry (DSC) measurements of **2**, recorded at $10 \text{ K}\cdot\text{min}^{-1}$, was also used over the temperature range 108–300 K in cooling and warming modes. As a result, a first-order phase transition was identified revealing in addition a hysteresis loop with $T_{\text{max}}^\uparrow = 171$ K and $T_{\text{max}}^\downarrow = 151$ K (Fig. 1b). The hysteresis loop width of 20 K exactly matches the one found by ^{57}Fe Mössbauer spectroscopy and SQUID magnetometry. The slight temperature shift (2 K) in the hysteresis loop is due to the higher scan rate compared to other measurements. Enthalpy and entropy associated to the SCO were evaluated as $\Delta H_{\text{SCO}} = 10.5 \text{ kJ}\cdot\text{mol}^{-1}$ and $\Delta S_{\text{SCO}} = 65.6 \text{ J}\cdot\text{mol}^{-1} \text{ K}^{-1}$.

The cooperativity strength of **2** has been evaluated in the framework of the widely used Slichter and Drickamer model, that uses a mean-field interaction parameter Γ [21].

Fig. 3 Thermal dependence of the HS fraction, γ_{HS} , measured (open circles) and simulated (full circles)



The best fit to the experimental curve (Fig. 3) was obtained with the following parameters: $\Gamma = 3.3 \text{ kJmol}^{-1}$, $\Delta H = 10.54 \text{ kJmol}^{-1}$, $\Delta S = 65.54 \text{ Jmol}^{-1}\text{K}^{-1}$. An excellent correspondence was found with the experimental thermodynamical parameters.

4 Conclusions

The spin transition of $[\text{Fe}\{\text{N}(\text{entz})_3\}_2](\text{ClO}_4)_2$ proceeds in a cooperative and complete fashion. Compared to $[\text{Fe}\{\text{N}(\text{entz})_3\}_2](\text{BF}_4)_2$, the hysteresis is wider, presumably due to the presence of an extended H-bonding network, as recently observed by single crystal X-ray diffraction in our laboratory. Nanostructuring of this material is under consideration for possible implementation of 2D switchable networks into memory devices [22].

Acknowledgements We acknowledge support from the the Fonds de la Recherche Scientifique-FNRS (PDR T.0102.15), WBI-Romanian Academy, CNCS-UEFISCDI, project number PN-II-RU-TE-2014-4-2695 (Contract No. 267/01.10.2015) and COST actions CM1305 and CA15128. M. M. D. is recipient of the GFSM 2016 thesis prize, and chargé de recherches from the F.R.S. - FNRS.

References

- Gütlich, P., Gaspar, A.B., Garcia, Y.: Spin state switching in iron coordination compounds. *Beilstein J. Org. Chem.* **9**, 342 (2013)
- Garcia, Y., Adarsh, N.N., Naik, A.D.: Crystal engineering of Fe^{II} spin crossover coordination polymers derived from triazole or tetrazole ligands. *Chimia* **67**, 411 (2013)
- Garcia, Y., Ksenofontov, V., Gütlich, P.: Spin transition molecular materials: new sensors. *Hyperfine Interact.* **139/140**, 543 (2002)
- Linares, J., Codjovi, E., Garcia, Y.: Pressure and temperature spin crossover sensors with optical detection. *Sensors* **12**, 4479 (2012)
- Vreugdenhil, W., van Diemen, J.A., de Graaff, R.A.G., Haasnoot, J.G., Reedijk, J., van der Kraan, A.M., Kahn, O., Zarembowitch, J.: HS-LS transition in $[\text{Fe}(\text{NCS})_2(4,4'\text{-bis-1,2,4-triazole})_2]\cdot\text{H}_2\text{O}$. X-ray crystal structure and magnetic, Mössbauer and EPR properties. *Polyhedron* **9**, 2971 (1990)
- Ozarowski, A., Shunzhong, Y., McGarvey, B.R., Mislankar, A., Drake, J.E.: EPR and NMR study of the spin crossover transition in bis(4,4'-bi-1,2,4-triazole)bis(thiocyanato)iron hydrate and bis(4,4'-bi-1,2,4-triazole)bis(selenocyanato)iron hydrate. X-ray structure determination of $\text{Fe}(4,4'\text{-bi-1,2,4-triazole})_2(\text{SeCN})\cdot\text{H}_2\text{O}$. *Inorg. Chem.* **30**, 3167 (1991)
- Chuang, Y.-C., Liu, C.-T., Sheu, C.-F., Ho, W.-L., Lee, G.-H., Wang, C.-C., Wang, Y.: New iron(II) spin crossover coordination polymers $[\text{Fe}(\mu\text{-atrz})_3]\text{X}_2\cdot 2\text{H}_2\text{O}$ ($\text{X} = \text{ClO}_4^-, \text{BF}_4^-$) and $[\text{Fe}(\mu\text{-atrz})(\mu\text{-pyz})(\text{NCS})_2]\cdot 4\text{H}_2\text{O}$ with an interesting solvent effect. *Inorg. Chem.* **51**, 4663 (2012)

8. Bronisz, R.: 1,4-di(1,2,3-triazol-1-yl)butane as building block for the preparation of the iron(II) spin crossover 2D coordination polymer. *Inorg. Chem.* **44**, 4463 (2005)
9. Kusz, J., Bronisz, R., Zubko, M., Bednarek, G.: On the role of intermolecular interactions on structural and spin crossover properties of 2D coordination networks, $[\text{Fe}(\text{bbtr})_3]_n \text{A}_n$ (bbtr = 1,4-bis(1,2,3-triazol-1-yl)butane; $\text{A} = \text{ClO}_4^-, \text{BF}_4^-$). *Chem. Eur. J.* **17**, 6807 (2011)
10. Quesada, M., Prins, F., Roubeau, O., Gamez, P., Teat, S.J., van Koningsbruggen, P.J., Haasnoot, J.G., Reedijk, J.: A 2D $[\text{Fe}^{\text{II}}\text{-bistetrazole}]$ coordination polymer exhibiting spin crossover properties *Inorg. Chim. Acta* **360**, 3787 (2007)
11. Bialonska, A., Bronisz, R.: HS and spin crossover 2D coordination polymers containing $\text{Fe}^{\text{II}}(\text{tetrazol-2-yl})_4(\text{soln})_2$ (soln = Ethanol, Acetonitrile) cores linked by flexible/elastic spacers. *Inorg. Chem.* **49**, 4534 (2010)
12. Ksiazek, M., Kusz, J., Bialonska, A., Bronisz, R., Weselski, M.: Influence of conformational changes on spin crossover properties and superstructure formation in 2D coordination polymers $[\text{Fe}(\text{hbtz})_2(\text{RCN})_2](\text{ClO}_4)_2$. *Dalton Trans.* **44**, 18563 (2015)
13. Bialonska, A., Bronisz, R., Kusz, J., Zubko, M.: Two-step spin transition in an iron(II) coordination network based on flexible bitopic ligand 1-(tetrazol-1-yl)-3-(1,2,3-triazol-1-yl)propane. *Eur. J. Inorg. Chem.* **5–6**, 884 (2013)
14. Bronisz, R., Ciunik, Z., Drabent, K., Rudolf, M.F.: New type of 2-D nets in iron(II) spin crossover systems - $[\text{Fe}\{\text{N}(\text{entz})_3\}_2](\text{BF}_4)_2$. *Conf. Proc., ICAME-95* **50**, 15 (1996)
15. Boland, Y., Herstens, P., Marchand-Brynaert, J., Garcia, Y.: New ditopic and tripodal 1,2,4-triazole- and tetrazole-based ligands for coordination chemistry. *Synthesis* **9**, 1504 (2006)
16. Bialonska, A., Bronisz, R., Rudolf, M.F., Weselski, M.: HSLs transition in Iron(II) 2D coordination networks containing tris(tetrazol-1-ylmethyl)methane as triconnected building block. *Inorg. Chem.* **51**, 237 (2012)
17. Kamiya, T., Saito, Y.: Process for preparing 1H-tetrazole compounds. US 3767667 A (1973)
18. Lagarec, K., Rancourt, D.G.: Mössbauer Spectral Analysis Software for Windows 1.0. Department of Physics, University of Ottawa, Canada (1998)
19. Rotaru, A., Dîrtu, M.M., Enachescu, C., Tanasa, R., Linares, J., Stancu, A., Garcia, Y.: Calorimetric measurements of diluted spin crossover complexes $[\text{Fe}_x\text{M}_{1-x}(\text{btr})_2(\text{NCS})_2] \cdot \text{H}_2\text{O}$ with $\text{M}^{\text{II}} = \text{Fe}$ and Ni. *Polyhedron* **28**, 2531 (2009)
20. Garcia, Y., Ksenofontov, V., Gütllich, P.: New polynuclear 4,4'-bis-1,2,4-triazole Fe^{II} spin crossover compounds. *C. R. Acad. Sci. Chim. IIC* **4**, 227 (2001)
21. Slichter, C.P., Drickamer, H.G.: Pressure-induced electronic changes in compounds of iron. *J. Chem. Phys.* **56**, 2142–2160 (1972)
22. Suarez-Garcia, S., Adarsh, N.N., Molnar, G., Bousseksou, A., Garcia, Y., Dîrtu, M.M., Pobles, R., Ordejón, P., Ruiz-Molina, D.: Spin crossover on an exfoliated 2-D coordination polymer (submitted) (2017)